Journal of Applied Mechanics and Technical Physics, Vol. 38, No. 2, 1997

NATURAL VIBRATIONS OF A UNIFORM CASCADE OF HYDRAULIC-TURBINE BLADES IN A FLUID

V. B. Kurzin, S. N. Korobeinikov, V. P. Ryabchenko, and L. A. Tkacheva

UDC 533.6

During operation, hydraulic-turbine blades are inevitably subjected to unsteady flow action, which induces forced vibrations of the blades. If the frequencies of the initiating forces are close to the natural frequencies of the blades, resonance can occur. This frequently causes blade failure in the operation of turbines. The above circumstances lead to the necessity of increasing the accuracy of calculation of eigenfrequencies and eigenmodes of blade vibrations. The difficulties in achieving this goal are due to a large number of factors that influence the solution of the corresponding hydroelastic problem, in which elastic deformations of blades and fluid motion should be determined simultaneously.

In most of the former papers devoted to this problem, these factors were not taken into account. Thus. Gorelov and Guseva [1] did not take into account the curvature of the blade surface, and also determined approximately (in a two-dimensional formulation) the hydrodynamic interaction. Naumenko et al. [2] studied a blade model in the form of a plate of variable thickness. Sundqvist [3] considered this problem for a blade model in the form of a variable-thickness shell in the most complete approximation and with allowance for spatial flow. However, the finite element method (FEM) employed in [3] to describe motion of both solid and fluid particles requires a large computer memory and time, and this limits the possibilities of the method in engineering practice.

The present work seeks to develop a method for calculating the natural vibrations of blades using a sufficiently general model similar to [3], which can be realized on personal computers. For this, to determine the hydrodynamic loads acting on the blades, we used the integral equation method, which decreased by unity the dimension of the corresponding hydrodynamic problem.

1. Basic Assumptions and Formulation of the Problem. We consider the problem of small free linear vibrations of rotor blades (Fig. 1) of an axial hydraulic turbine in a fluid. The rotor is simulated by an annular cascade consisting of N identical, fairly thin blades located between two infinite circular cylinders with radii R_1 and R_2. We assume that the interaction between the blades occurs only via the fluid, which is ideal and incompressible and whose motion is caused only by blade vibrations.

By virtue of the assumption of small blade thickness, we write the problem for the displacements of the centroidal surfaces. According to the condition of cascade uniformity [4], the normal vibrations of the centroidal surfaces can be written as

$$w_m^j = u_m^j(\mathbf{x})e^{i(\omega_j + \mu_j m)} \quad (j, m = 0, 1, 2, \ldots, N-1). \tag{1.1}$$

Here $\mu_j = 2\pi j/N$ is the phase shift between vibrations of neighboring blades, ω_j is the eigenfrequency of blade vibrations with a phase shift μ_j, u_m^j is an amplitude function of the displacement of the centroidal surface S_m of the mth blade, and $\mathbf{x}$ is the radius vector of the points on the surface S_m.

Taking into account (1.1), we can reduce the equation of the normal vibrations of the blade cascade with allowance for their hydrodynamic interaction to the following matrix equations:

Lavrent'ev Institute of Hydrodynamics, Siberian Division, Russian Academy of Sciences, Novosibirsk 630090. Translated from Prikladnaya Mekhanika i Tekhnicheskaya Fizika, Vol. 38, No. 2, pp. 80–90, March–April, 1997. Original article submitted August 31, 1995; revision submitted July 21, 1995.

 0021-8944/97/3802-0240 $18.00 © 1997 Plenum Publishing Corporation

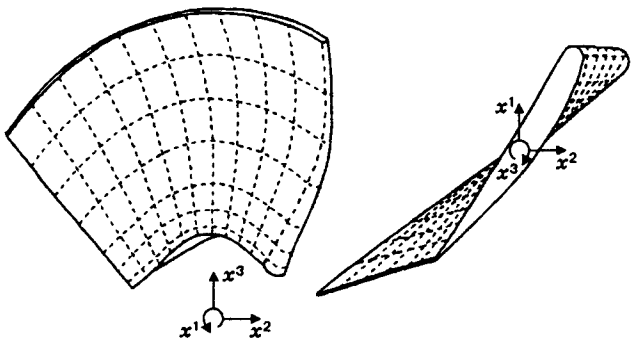

Fig. 1

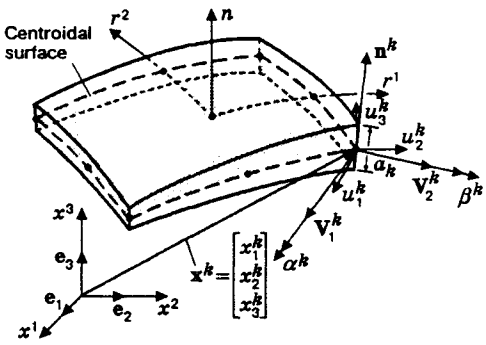

Fig. 2

$$[C - \lambda_j(M + A_j)]\mathbf{X}_j = 0, \qquad \lambda_j = \omega_j^2 \quad (j = 0, 1, 2, \ldots, N-1). \tag{1.2}$$

Here

$$A_j = \sum_{s=0}^{N-1} L_s \, e^{i\mu_j s};$$

$s = n-m$ for $n \geqslant m$; $s = N+(n-m)$ for $n < m$, L_s are the matrices of the hydrodynamic influence coefficients of the generalized displacements of the nth blade on the generalized hydrodynamic forces acting on the mth blade, C and M are the stiffness and mass matrices, and $\mathbf{X}_j$ is the vector of the coefficients of approximation of the amplitude function u_m^j of the initial blade ($m = 0$) over a system of basis functions. It is required to determine the eigenvalues of the matrix equation (1.2). For this, it is necessary to choose preliminarily a system of basis functions, to construct stiffness and mass matrices, and to determine hydrodynamic loads acting on the vibrating blades.

2. Use of the FEM to Determine Stiffness and Mass Matrices. At present, there are many formulations of shell finite elements to calculate the strength and vibrations of thin-walled structures. Among these of great interest is the formulation of an isoparametric shell finite element obtained by direct introduction of kinematic and static hypotheses of shell theory into the three-dimensional theory of elasticity [5, 6]:

- a filament which initially coincides with the normal vector to the centroidal shell surface remains straight during deformation and its length does not change (Timoshenko's kinematic hypothesis);
- the stresses in the normal direction to the centroidal surface of the shell are negligible compared with the other components of the stress tensor.

Since in the construction of this element, no additional restrictions, besides the two mentioned above, are imposed on the equations of elasticity theory, the finite element can be used to calculate nonshallow shells and variable-thickness shells. The turbine blades are among this class of shells, and, hence, the element can be naturally used to calculate strains of such structures.

Korobeinikov [7] proposed a nonlinear formulation of the above-described isoparametric element. Element approximations ranging from linear to cubic are used. The element stiffness matrix is constructed so that separate integration of the membrane and displacement terms is possible [5]. This element is included in the finite-element library of the PIONEER program [8].

Using an isoparametric finite shell element [7], we derive expressions for the stiffness C and mass M matrices which are required to solve the problem of vibrations of hydraulic-turbine blades in a fluid. Since we study linear vibrations of the blade, the matrix C is defined in a linear formulation. We consider a certain finite element (Fig. 2). As a reference system we use Cartesian coordinates (x^1, x^2, x^3) with unit vectors $\mathbf{e}_1$, $\mathbf{e}_2$, and $\mathbf{e}_3$. Let r^1 and r^2 be natural coordinates on the centroidal surface of the shell element, and n the coordinate in the normal direction to the centroidal surface of the shell (Fig. 2). Note that the coordinate system (r^1, r^2, n) is not orthogonal in the general case. Using Timoshenko's kinematic hypothesis, we can

write the displacement vector of a material point on the shell element as [5, 6]

$$\mathbf{u} = \sum_{k=1}^{K} h_k \mathbf{u}^k + \frac{n}{2} \sum_{k=1}^{K} a_k h_k (-\alpha^k \mathbf{V}_2^k + \beta^k \mathbf{V}_1^k), \tag{2.1}$$

where $h_k = h_k(r^1, r^2)$ are interpolation polynomials; $\mathbf{u}^k$ is the displacement vector of the nodal point k, a_k is the shell thickness at the nodal point k, $\mathbf{V}_1^k$ and $\mathbf{V}_2^k$ are orthogonal unit vectors in the centroidal surface of the shell to the nodal point k, which can be constructed, for example, by the formulas proposed in [5, 6], α^k and β^k are small rotations of the normal unit vector $\mathbf{n}^k$ around the vectors $\mathbf{V}_1^k$ and $\mathbf{V}_2^k$, respectively (Fig. 2), and the superscript and subscript k takes on values from 1 to K, where K is the number of nodal points in the element.

The strain-tensor components are written as

$$e_{ij} = \frac{1}{2}(u_{i,j} + u_{j,i}). \tag{2.2}$$

The subscript after the comma denotes the partial derivative with respect to the corresponding coordinate.

We introduce the vector of nodal displacements of the element:

$$\mathbf{u}^e = \left[u_1^1, u_2^1, u_3^1, \alpha^1, \beta^1, \ldots, u_1^K, u_2^K, u_3^K, \alpha^K, \beta^K\right]^{\mathrm{t}} \tag{2.3}$$

(the superscript t denotes transposition). We also introduce a vector composed of the strain-tensor components:

$$\mathbf{e} = [e_{11}, e_{22}, e_{33}, 2e_{12}, 2e_{13}, 2e_{23}]^{\mathrm{t}}. \tag{2.4}$$

Using (2.1) and notation of (2.3) and (2.4), we can write relations (2.2) in matrix-vector form as

$$\mathbf{e} = B\,\mathbf{u}^e. \tag{2.5}$$

The components of matrix B are given in [6].

To take into account the equality to zero of the stress component in the normal direction to the centroidal surface, we introduce a local coordinate system $(\hat{x}^1, \hat{x}^2, \hat{x}^3)$ of the layer with orthogonal basis vectors $\hat{\mathbf{e}}_1$, $\hat{\mathbf{e}}_2$, and $\hat{\mathbf{e}}_3$ so that the unit vectors $\hat{\mathbf{e}}_1$ and $\hat{\mathbf{e}}_2$ are in the plane $n = \text{const}$, and the unit vector $\hat{\mathbf{e}}_3$ is directed normal to this plane. To avoid confusion, note that basis unit vectors $\mathbf{V}_1^k$, $\mathbf{V}_2^k$, and $\mathbf{n}^k$ are introduced at the nodal point of the *centroidal surface* of the element, and the basis unit vectors $\hat{\mathbf{e}}_1$, $\hat{\mathbf{e}}_2$, and $\hat{\mathbf{e}}_3$ are constructed at the integration points over the element volume. We introduce a vector composed of the strain-tensor components (the component $\hat{e}_{33}$ is excluded from consideration because of the assumption of equality to zero of the corresponding stress tensor component): $\hat{\mathbf{e}} = [\hat{e}_{11}, \hat{e}_{22}, 2\hat{e}_{12}, 2\hat{e}_{13}, 2\hat{e}_{23}]^{\mathrm{t}}$ (the superscript hat denotes the components of the corresponding vector or tensor in the coordinate system of the layer). Let Q be the matrix of transformation of the vector composed of the strain-tensor components in the Cartesian coordinate system (x^1, x^2, x^3) to the vector composed of the strain-tensor components in the coordinate system of the layer $(\hat{x}^1, \hat{x}^2, \hat{x}^3)$:

$$\hat{\mathbf{e}} = Q\,\mathbf{e}. \tag{2.6}$$

The elements of the matrix Q are found by the usual rules of transformation of the tensor components from one coordinate system to another. Substituting (2.5) into (2.6), we obtain $\hat{\mathbf{e}} = \hat{B}\mathbf{u}^e$ and $\hat{B} = QB$.

Let us introduce a vector composed of the stress tensor components $\hat{\sigma}_{ij}$ in the layer coordinate system $(\hat{x}^1, \hat{x}^2, \hat{x}^3)$ (satisfaction of the equality $\hat{\sigma}_{33} = 0$ by virtue of the adopted static hypothesis is assumed): $\hat{\boldsymbol{\sigma}} = [\hat{\sigma}_{11}, \hat{\sigma}_{22}, 2\hat{\sigma}_{12}, 2\hat{\sigma}_{13}, 2\hat{\sigma}_{23}]^{\mathrm{t}}$. The governing relations for a linear isotropic elastic body are written as

$\hat{\sigma} = \hat{D}\,\hat{\mathrm{e}}$, where the matrix [5] is

$$\hat{D} = \frac{E}{1-\nu^2}\begin{bmatrix} 1 & \nu & 0 & 0 & 0 \\ \nu & 1 & 0 & 0 & 0 \\ 0 & 0 & (1-\nu)/2 & 0 & 0 \\ 0 & 0 & 0 & \hat{k}(1-\nu)/2 & 0 \\ 0 & 0 & 0 & 0 & \hat{k}(1-\nu)/2 \end{bmatrix}.$$

Here E is the Young modulus, ν is the Poisson ratio, and $\hat{k}$ is a correcting factor. Direct use of Timoshenko's kinematic hypothesis in the case of elastic deformation leads to a linear stress distribution across the shell thickness. This circumstance contradicts the fact that the shear stress components $\hat{\sigma}_{13}$ and $\hat{\sigma}_{23}$ should be equal to zero on the face surfaces of the shell. The latter condition is satisfied with a parabolic distribution of these shear stress components across the shell thickness. The parabolic distribution law of the shear stress components is satisfied in an energetic sense when the correcting factor $\hat{k} = 5/6$ is used [5]. In the present work, we used this value of the factor $\hat{k}$. According to the standard FEM, the stiffness matrix of a shell finite element is given by the formula [5, 6]

$$C^e = \int_{V^e} \hat{B}^{\mathrm{t}} \hat{D}\,\hat{B}\,dV, \tag{2.7}$$

where V^e is the volume of the finite element.

From (2.1) and (2.3) we obtain the relation $\mathbf{u} = H\,\mathbf{u}^e$, where the elements of the matrix H have the form

$$H = \left[\begin{array}{c|ccccc|c} & h_k & 0 & 0 & nh_k g_{11}^k & nh_k g_{21}^k & \\ \ldots & 0 & h_k & 0 & nh_k g_{12}^k & nh_k g_{22}^k & \ldots \\ & 0 & 0 & h_k & nh_k g_{13}^k & nh_k g_{23}^k & \end{array}\right].$$

Here $g_{1i}^k = -(a_k/2)V_{2i}^k$ and $g_{2i}^k = (a_k/2)V_{1i}^k$.

According to the standard FEM technique, we write a consistent mass matrix for the element [5, 6]:

$$M^e = \int_{V^e} H^{\mathrm{t}} H \rho_s\,dV, \tag{2.8}$$

where ρ_s is the mass density of the shell material.

The stiffness matrix (2.7) and the mass matrix (2.8) are integrated over the volume of the elements numerically by means of the Gauss–Legendre quadrature formulas. The stiffness matrix can be integrated with the full order or a reduced order, or using the rule of selective integration of membrane and shear terms [5, 6]. The full integration order depends on the degree of the interpolation polynomials $h_k(r^1, r^2)$. For example, when the full biquadratic approximation of the geometry and vector of the unknown displacements of the centroidal surface of the element ($K = 9$) and a linear approximation over the element thickness (linear approximation over the element thickness is consistent with Timoshenko's kinematical hypothesis) are used. the full integration order of the stiffness matrix with respect to the coordinates r^1, r^2, and n by means of the Gauss–Legendre quadrature formula is $3 \times 3 \times 2$ [6]. In this case, the total number of the integration points in the element is 18. With a reduced integration order, $2 \times 2 \times 2$ quadrature points are used. In selective integration of the stiffness matrix of the 9th nodal finite element, the membrane terms are integrated with $3 \times 3 \times 2$ order and the shear terms with $2 \times 2 \times 2$ order. In using reduced and selective orders of integration. we obtain a more rapid convergence to the exact solution for thin shells than in using the full integration order [5, 6]. However, this is not always possible because of the occurrence of spurious zero eigenmodes, and this integration cannot be performed for all edge constraints of the shell.

Summing up the stiffness matrix and the mass matrix of the elements by the usual procedure [5, 6], we obtain the global stiffness matrix C and the mass matrix M of the entire finite-element ensemble.

3. Determination of Hydrodynamic Loads on Blades. We consider an annular cascade of N blades in Cartesian coordinates (x^1, x^2, x^3). The blades vibrate in an ideal incompressible fluid between two

infinite coaxial circular cylinders C_1 and C_2 with radii R_1 and R_2, respectively. The x^1 axis is directed along the cylinder axis. We assume that at infinite distance from the cascade, the fluid is at rest, and the flow past the blades is not separated. Under the conditions of the problem, the cascade blades are sufficiently thin. Therefore, to determine the hydrodynamic loads, the blades can be simulated by infinitely thin surfaces S_n $(n = 1, 2, \ldots, N)$ that coincide with the centroidal surfaces of the blades considered.

Since the amplitude of the vibrations is small, the fluid flow is potential. To describe it, we can introduce the function Φ that is related to the fluid-velocity potential φ by $\varphi = iR_2^2\omega\Phi(\mathbf{x})\,e^{i\omega t}$, where $\mathbf{x} = [x^1, x^2, x^3]^t$.

The function Φ satisfies the Laplace equation everywhere outside the blades and is subjected to the boundary conditions of nonpenetration on the surfaces S_n and cylinders C_1 and C_2 and to the condition that perturbations decay with distance from the cascade. By virtue of the fact that the leading and trailing edges of the blades are under identical conditions, we seek a solution of the problem in the class of circulation-free flows. A vortex sheet does not form behind the blades, since the fluid-velocity circulation around any contour embracing the blade in the radial cross section is equal to zero.

We replace the cascade blades S_n and the cylinders C_1 and C_2 by vortex surfaces and introduce the velocity rotor on the surface S_n in the form $\gamma = \mathbf{n} \times [\mathbf{v}]$, where $\mathbf{n}$ is a unit normal vector to the surface and $[\mathbf{v}]$ is the velocity jump across S_n. The fluid-flow velocity induced by these vortices is given by the Biot–Savart formula

$$\mathbf{v}(\mathbf{x}) = \nabla\Phi = -\int_{S_n} \gamma \times \nabla_{\mathbf{y}} G\, dS, \qquad G = 1/(4\pi|\mathbf{x} - \mathbf{y}|).$$

Here $\mathbf{y} = [y^1, y^2, y^3]^t$ is the radius vector of a point on the surface S_n and $\nabla_{\mathbf{y}} G$ is the gradient of the function G calculated with respect to the vector $\mathbf{y}$. Here and below the quantities that have the dimension of length are related to the radius R_2 of the external cylinder. The nonpenetration condition gives a system of integral equations for the vector γ. The perturbed velocities decay with distance from the cascade because of the choice of the fundamental solution G. Since the blades vibrate with a constant phase shift, and perturbations decay with distance from the lattice, it will suffice to consider the surface parts of the cylinders C_1 and C_2 with length L along the x^1 axis and with size $2\pi/N$ along the angular coordinate in the plane $x^1 = \text{const}$. The circulation-free fluid flow is ensured in going to the discrete analog of the problem. The resulting system of integral equations is solved by the method of discrete vortices. As the main discrete element, we choose a closed trapezoidal vortex frame. The circulations along the sides of the frame are equal and constant in magnitude, and their sum is equal to zero [9]. The method of vortex frames for calculating circulation-free flow past finite-span wings of finite amplitude is described in [10]. Since the circulation Γ along one side of the frame is constant, we have

$$\gamma\, dS = \Gamma \frac{\partial \mathbf{y}}{\partial s}\, ds,$$

where s is a variable along this line. In this case, the integrals along the sides are calculated analytically. For an annular cascade, it is convenient to introduce two directions lying in the tangential plane to the surface considered (blades or cylinders):

(1) in the direction of the radius r,

(2) along the tangent τ to the line of section of the blade for $r = \text{const}$.

The vortex frame Π_{ki} with circulation $\Gamma_{ki} = \Gamma(\mathbf{x}^0_{ki})$ ($\mathbf{x}^0_{ki}$ is the radius vector of the middle of the vortex segment $[A_{k,i}; A_{k+1,i}]$) consists of vortex segments $[A_{k,i}; A_{k+1,i}]$, $[A_{k+1,i}; A_{k+1,i+1}]$, $[A_{k+1,i+1}; A_{k,i+1}]$, and $[A_{k,i+1}; A_{k,i}]$ ($k = \overline{1, N_1}$ and $i = \overline{1, N_2}$, where N_1 is the number of partitions over r and N_2 is the number of partitions over τ). Integers 1 and 2 in Fig. 3 denote, respectively, the control points and points at which the pressure jump is calculated, and integer 3 denotes the nodes of the finite element.

Then, the component γ_r of the vector γ (intensity of bound vortices), which is necessary in determining the pressure jump across the blade, has the form $\gamma_r(\mathbf{x}^0_{ki}) = (\Gamma_{ki} - \Gamma_{k,i-1})/\delta\tau$ since the segment $[A_{k,i}; A_{k+1,i}]$ enters into the neighboring vortex frames $\Pi_{k,i-1}$ and Π_{ki} with different circulation signs. Here $\delta\tau$ is the width of the vortex frame. In this case, since the flow is circulation-free, we assume that the circulations of the vortex frames at the trailing edge of the blade are equal to zero.

By virtue of the aforesaid, the determination of the circulation of the vortex frame of the blade $\Gamma = \{\Gamma_{ki}\}$ and the cylinders $\Gamma_1 = \{\Gamma_{1mn}\}$ reduces to solution of the following system of linear algebraic equations: $W(\mathbf{x},\mathbf{x})\,\Gamma + W_1(\mathbf{x},\mathbf{y})\,\Gamma_1 = \mathbf{F}$ and $W(\mathbf{y},\mathbf{x})\,\Gamma + W_1(\mathbf{y},\mathbf{y})\,\Gamma_1 = 0$. Here $\mathbf{x}$ and $\mathbf{y}$ ate the radius vectors of points on the blade and on the cylinders C_1 and C_2, W is the matrix of the normal velocity components induced by the vortex frames of the blade with unit circulation at points on the blade $[W(\mathbf{x},\mathbf{x})]$ or at points on the cylinders C_1 and C_2 $[(\mathrm{W}(\mathbf{y},\mathbf{x})]$; W_1 is a similar matrix for the normal velocities of the vortex frame modeling the effect of the cylinders C_1 and C_2 at points on the blade $[W_1(\mathbf{x},\mathbf{y})]$ and at points on the cylinders $[W_1(\mathbf{y},\mathbf{y})]$, and $\mathbf{F}$ is the vector of the amplitudes of the normal velocity component of blade vibrations. Multiplying the second equation of the system from the left by $W_1^{-1}(\mathbf{y},\mathbf{y})$ and substituting the vector Γ_1 into the first equation, we find the circulations of the vortex frames of the blade: $\Gamma = T^{-1}\mathbf{F}$ and $T = W(\mathbf{x},\mathbf{x}) - W_1(\mathbf{x},\mathbf{y})[W_1^{-1}(\mathbf{y},\mathbf{y})\,W(\mathbf{y},\mathbf{x})]$. Note that this algorithm is more effective if in determining the velocities induced by the vortex frames of the blades at points of the cylinders, one draws their reflection with respect to the cylinders C_1 and C_2 at each cross section $x^1 = \text{const}$.

To determine nonstationary hydrodynamic loads, we use the Joukowski theorem for circulation-free flow, according to which the pressure jump is given by the formula

$$[p] = \rho_f \frac{\partial \Gamma_c}{\partial t}, \quad \Gamma_c = \int\limits_{C(M)} \mathbf{n} \times \boldsymbol{\gamma}\, d\mathbf{x},$$

where $[p] = p_- - p_+$ and ρ_f is the fluid mass density. The curve $C(M)$ is drawn on the vortex surface of the blade from the leading edge to point M at which the pressure difference is determined.

The discrete analog of these relations has the form

$$p_{jm} = \sum_{k=1}^{m} g_{jk}, \quad g_{j1} = \Gamma_{j1}, \quad g_{jN_2} = -\Gamma_{j,N_2-1},$$

$$g_{jk} = \Gamma_{jk} - \Gamma_{j,k-1} \quad \text{for} \quad k \neq 1, k \neq N_2 \quad (j = \overline{1, N_1}, \quad m = \overline{1, N_2}).$$

Here p_{jm} is the pressure jump in the middle of the bound vortices of the vortex frame. These formula take into account that the circulations of the vortex frames on the left and right edges of the blade vanish.

4. Algorithm of Solution for the Eigenvalue Problem. The solution of the corresponding hydrodynamic problem by the method of integral equations, besides the above-mentioned advantages, involve difficulties in determining the matrices A_j since the basis functions of the elastic deformations of the blade are consistent with the FEM. In this case, to construct the matrices A_j, it would be required to solve the corresponding hydrodynamic problem for different linear independent blade-vibration modes as many times as the number of finite elements used to describe the blade deformation as a whole. A specific feature of the proposed algorithm is that the iterative method of solving the eigenvalue problem allows one to eliminate calculation of the matrices A_j in explicit form. Indeed, the matrix enters into Eq. (1.2) only as a product by the vector $\mathbf{X}_j$, which is the vector of the hydrodynamic load on the blade $\mathbf{P}_j = A_j\mathbf{X}_j$. In the nth step of the iteration process described below, this vector is determined by solution of the hydrodynamic problem formulated in Sec. 3 with the given vibration mode found in the previous step. Solution of this problem immediately gives the hydrodynamic pressure difference $[p_j]$ on the centroidal surface of the blade. The load vector $\mathbf{P}_j^e$ acting on a certain element on the centroidal surface S^e is related to the pressure jump on it by

$$\mathbf{P}_j^e = \int\limits_{S^e} [p_j] H^{\mathrm{t}} \mathbf{n}\, dS, \tag{4.1}$$

where H is the matrix defined in Sec. 2. The global vector $\mathbf{P}_j$ is obtained by the usual summation rule [6] for the vectors of nodal loads of all elements.

Gaussian–Legendre quadrature formulas were used in the numerical integration of (4.1). Since finite element integration points do not coincide with the nodal points in the method of integral equations, interpolation was performed to obtain the pressure jump at the required points. We used linear interpolation, since the pressure-jump function does not show required smoothness near the leading and trailing edges. The

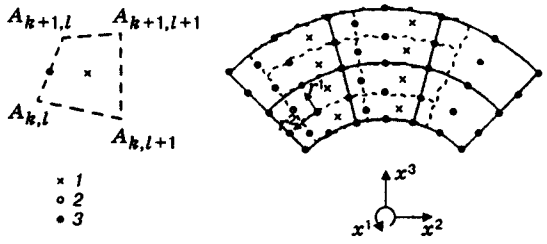

Fig. 3

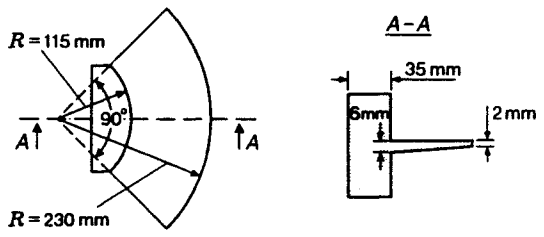

Fig. 4

relative location of the finite elements and the vortex frames is shown in Fig. 3.

The eigenmodes of blade vibrations in vacuum were used as the initial approximation. The experimental and calculated data indicate that the eigenmodes of blade vibrations of three lower tones in fluid are close to the corresponding modes of blade vibrations in vacuum. Therefore, the convergence of the iteration process is very good, as confirmed by the calculations. Since the blade-vibration modes of lower tones have a small number of nodal lines, the hydrodynamic problem can be solved iteratively with a relatively small number of vortex frames.

The iteration process is performed as follows. Using the Cholesky factorization for the stiffness matrix $C = LL^{\mathrm{t}}$ (L is the lower triangular matrix), we perform a transformation of Eq. (1.2):

$$[\eta_j J - L^{-1}(M + A_j)(L^{\mathrm{t}})^{-1}]\mathbf{Y}_j = 0,$$

where $\eta_j = 1/\lambda_j$, $\mathbf{Y}_j = L^{\mathrm{t}}\mathbf{X}_j$, and J is a unit matrix. As a result, we obtain the eigenvalue problem for the Hermitian matrix:

$$G_j = L^{-1}(M + A_j)(L^{\mathrm{t}})^{-1}. \tag{4.2}$$

According to [11], the first eigenvalue η_{1j} of the matrix G_j can be determined by the method of direct iterations of the form

$$\mathbf{Y}_j^{n+1} = G_j\mathbf{Y}_j^n / \|\mathbf{Y}_j^n\|_\infty, \tag{4.3}$$

where $\|\ \|_\infty$ is the norm in l_∞, i.e., the vector element with a maximum module. With allowance for (4.2), relation (4.3) becomes

$$\mathbf{Y}_j^{n+1} = [L^{-1}M(L^{\mathrm{t}})^{-1}\mathbf{Y}_j^n + L^{-1}\mathbf{P}_j^n] / \|\mathbf{Y}_j^n\|_\infty. \tag{4.4}$$

Here the matrix A_j is not contained. As the initial approximation of process (4.4), we use the eigenvector of blade vibrations in vacuum, which is determined by the subspace iterative method [6].

According to [11], this iteration process converges so that $\mathbf{Y}_j^n/\|\mathbf{Y}_j^n\|_\infty \to \mathbf{Y}_j/\|\mathbf{Y}_j\|_\infty$ and $\|\mathbf{Y}_j^n\|_\infty \to \eta_{1j}$ for $n \to \infty$. The convergence speed is given by the ratio η_{1j}/η_{2j}. Thus, if the eigenvalues η_{2j} and η_{1j} are close, the convergence speed is slow. It can be increased by means of a shift. In this case, the matrix $F_j = G_j - \zeta J$ has eigenvalues $\eta_{1j} - \zeta$, $\eta_{2j} - \zeta, \ldots$ and the same eigenvectors as the matrix G_j. The shift is chosen so that the eigenvalue $\eta_{2j} - \zeta$ has a maximum module and, at the same time, ratio (4.3) for the matrix F_j is smaller. To determine the subsequent eigenvalues, we use the exhausting method by means of unitary transformations [11].

5. Numerical Realization of the Algorithm and Comparison of the Calculation Results with Experimental Data. We developed an IBM PC/AT-486 computation program for eigenfrequencies and modes of blade vibration in a fluid under the assumption of blade clamping to realize numerically the algorithm of solution of the formulated problem. This specialized computation program was developed on the basis of the PIONER general-purpose program. During adjustment of the program, some difficulties arose in choosing test examples that would have reliable inlet information and reliable determination results for the required quantities, and also adequately reflect the generality of the posed problem. From this viewpoint, we chose the results obtained experimentally at the Leningrad Metal Plant in studies of the frequencies and modes of the eigenvibrations of a sectorial plate of variable thickness [12] and a PL 587B blade, which were

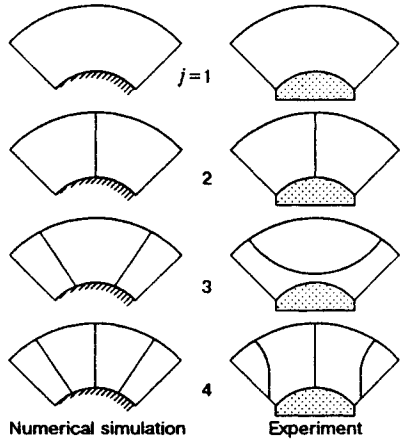

Fig. 5

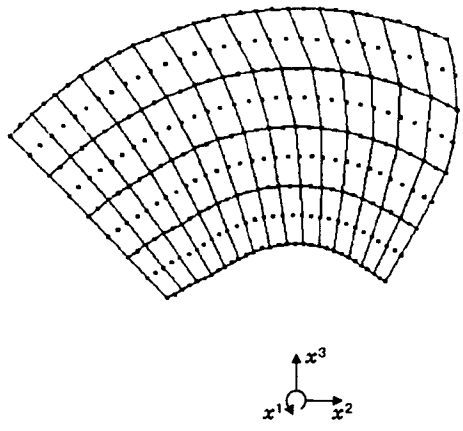

Fig. 6

TABLE 1

Tone number	f, Hz			
	Calculation			Experiment
	4×6 elements	4×9 elements	4×12 elements	
1	408	412	414	416
2	443	446	444	402
3	566	574	570	514
4	827	815	798	714

TABLE 2

Tone number	f, Hz			
	Calculation			Experiment
	4×6 elements	4×9 elements	4×12 elements	
1	140	144	145	159
2	212	212	209	—
3	329	320	314	277
4	545	450	486	420

kindly provided by V. A. Kovalenko and A. P. Nikiforov. The tests were performed by the resonance method. A sample in the form of a plate of variable thickness (its dimensions are given in Fig. 4) was fixed in a massive hub, which was suspended on a rubber membrane to a rigid bracket. A cylindrical shell that simulated the casing of the wheel was placed coaxially to the peripheral section of the specimen. An exciting force was applied to the hub with the sample and was directed along the axis of the suspension. The vibration modes were determined by the Lissajous figures. Experiments in water were performed with various water levels. Analysis of the results show that with a water layer above 75 mm the eigenfrequency of the specimen remains unchanged.

Tables 1 and 2 give the calculated eigenfrequencies $f = \omega/2\pi$ of the sectorial plate in vacuum and water, respectively, obtained for various numbers of blade finite elements, and their experimental values (the second vibration mode in fluid was not detected experimentally). The plate vibration modes in water practically did not differ from the corresponding modes in air in both the calculation and experiment. Figure 5 show the zero displacement lines of the first four vibration modes of the plate. Evidently, the calculated eigenfrequencies of the plate, except for the first tone, are somewhat higher than the experimental.

The eigenfrequencies and modes of blade vibrations for a PL 587B hydraulic turbine model were also calculated. In this case, the inlet data for the calculations were obtained with the mathematical blade model developed at the Institute of Mathematics, Siberian Division, Russian Academy of Sciences. The finite-element blade model is presented in Fig. 6. Table 3 gives the eigenfrequencies for a blade fastened to a hub. The slight difference between the calculated and experimental frequencies and vibration modes is obviously due to the fact that the calculated model does not take into account the actual clamping to the elastic hub for the blade and the sectorial plate.

As for the sectorial plate, the first three vibration modes (Fig. 7a–c, respectively) in vacuum and water

TABLE 3

Tone number	f, Hz			
	in vacuum		in water	
	Calcul.	Experim.	Calcul.	Experim.
1	789	705–761	456	408–498
2	1065	880–1068	705	612–770
3	1525	1412–1496	1124	957–1066

TABLE 4

Tone number	f, Hz					
	$\alpha = -10°$		$\alpha = 0$		$\alpha = 10°$	
	$\mu = 0$	$\mu = \pi$	$\mu = 0$	$\mu = \pi$	$\mu = 0$	$\mu = \pi$
1	467	448	471	448	473	448
2	709	700	714	700	716	699
3	1121	1122	1124	1122	1126	1122

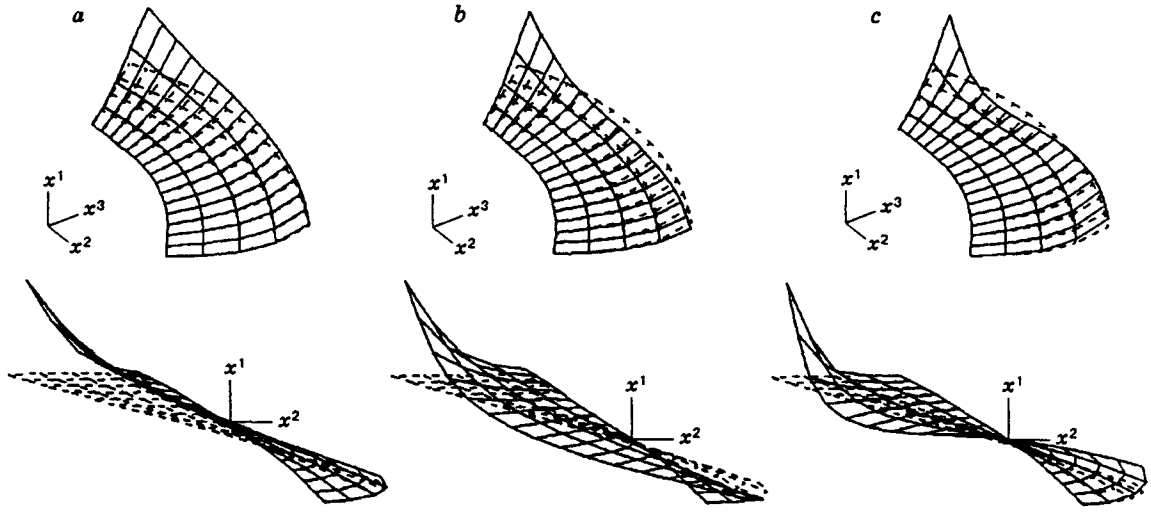

Fig. 7

practically do not differ from one another. The dashed curve is the initial position of the blade, and the solid curve is a deformed state. Since the eigenmodes are determined with accuracy up to a constant multiplier. the multiplier used is fairly large for better representation of the deformed structure in Fig. 7.

Table 4 gives the calculated eigenfrequencies for the same model but with a blade cascade with various stagger angles and phase shifts $\mu = 0$ and π. In this case, $\alpha = 0$ corresponds to the working position of the blade in the cascade, and $\alpha = \pm 10°$ corresponds to rotation from the initial position around the rotation axis of the blade. The results indicate that the phase shift has a greater effect, particularly on the first frequency. than the stagger angle.

The numerical experiment showed fast convergence of the iterative process in calculations of the eigenfrequencies and vibration modes. In the examples considered, the number of iterations depended on the tone number and did not exceed five. The iterative process was continued until the relative error of the eigenvector was 0.001. The computation time on an IBM PC/AT-486 (40 MHz) computer was 30 min.

This work was supported by the Russian Foundation for Fundamental Research (Grant No. 94-01-01220-a).

REFERENCES

1. D. N. Gorelov and L. A. Guseva, "Blade vibration of axial hydraulic turbines in a fluid flow," in: *Aeroelasticity of Turbomachines* (Collected scientific papers) [in Russian], Naukova Dumka, Kiev (1980), pp. 81–89.
2. V. V. Naumenko, V. G. Satsuk, E. A. Strelnikova, and V. A. Simonenko, "Method of discrete singularities in problems of free vibrations of hydraulic turbine blades in an ideal incompressible fluid," in: *Method of Discrete Singularities in Problems of Mathematical Physics and Its Role in the*

Development of a Numerical Computer Experiment: Abstracts III All-Union Symposium [in Russian], Izd. Khar'kov Univ., Khar'kov (1987), pp. 131–132.

3. J. Sundqvist, "An application of ADINA to the solution of fluid-structure interaction problems," *Comput. Struct.*, **17**, Nos. 5 and 6, 793–807 (1983).
4. D. N. Gorelov, V. B. Kurzin, and V. É. Saren, *Cascade Aerodynamics in Unsteady Flow* [in Russian], Nauka, Novosibirsk (1971).
5. O. Zienkiewicz and R. Taylor, *The Finite Element Method* (4th ed.), McGraw-Hill, London (1990).
6. K. J. Bathe, *Finite Element Procedures in Engineering Analysis*, Prentice–Hall, Englewood Cliffs, New Jersey (1982).
7. S. N. Korobeinikov, "Geometric nonlinear analysis of shells including large rotation increments," in: *Modeling in Mechanics* (Collected scientific papers) [in Russian], Inst. of Theor. and Appl. Mech.–Computational Center, Siberian Division, USSR Academy of Sciences, **4**, No. 4 (1990), pp. 119–126.
8. S. N. Korobeinikov, V. P Agapov, M. I. Bondarenko, and A. N. Soldatkin. "The general purpose nonlinear finite element structural analysis program PIONER," in: *Proc Int. Conf. on Numerical Methods and Applications*, Publ. House Bulg. Acad. Sci., Sofia (1989), pp. 228–233.
9. V. P. Ryabchenko, "Calculation of the associated mass of an annular blade cascade of arbitrary configuration by the discrete vortex method," in: *Tr. TsIAM: Aeroelasticity of Turbomachine Blades* [in Russian], **6**, No. 1293, Issue 6 (1991), pp. 79–86.
10. S. M. Belotserkovskii and I. K. Lifanov, *Numerical Methods in Singular Integral Equations and Their Applications in Aerodynamics, Theory of Elasticity, and Electrodynamics* [in Russian], Nauka, Moscow (1985).
11. J. Wilkinson, *The Algebraic Eigenvalue Problem*, Clarendon Press, Oxford (1965).
12. V. A. Kovalenko, S. N. Yavits, and V. G. Vinogradov, "An experimental study of the frequencies and modes of natural vibrations of a sector plate of variable thickness in air and water," in: *Engineering Information* No. 985, Leningrad Metal Plant, Leningrad (1980).